CONCEPT FOR FAST SPECTRAL CHARACTERISATION OF IMAGING SPECTROMETERS

Christian J. Schwarz, Karim Lenhard, and Peter Gege

German Aerospace Center, DLR, Remote Sensing Technology Institute, 82234 Wessling, Germany
christian.schwarz@dlr.de

ABSTRACT

For imaging spectrometers in the range of 350 - 2500 nm spectral characterization is accomplished currently at the Calibration Home Base (CHB) facility at DLR Oberpfaffenhofen using a Quartz-Tungsten-Halogen (QTH) lamp and a monochromator illuminating one pixel at a time. Here a new concept of spectral measurements is presented by making use of a laser driven optical parametric oscillator (OPO) tunable through the spectral region of 405 nm to 2550 nm allowing to characterize all of the pixels simultaneously. The advantages as speed of measurement due to higher spectral radiance, easier alignment and better spectral distribution of illumination are discussed.

Key words: spectral characterization; tunable laser; down conversion; imaging spectrometer; calibration.

1. INTRODUCTION AND MOTIVATION

Calibrating imaging spectrometers typically requires three types of measurements: radiometric, geometric and spectral characterization. In this paper spectral characterization of imaging spectrometers will be discussed for the future use at DLR's 'Calibration Home Base' (CHB), a laboratory configured for the characterization of airborne imaging spectrometers up to 500 kg and unique in Europe [1].

Currently at CHB a QTH lamp with a monochromator or pencil lamps are used for spectral characterization. Recently a laser driven optical parametric oscillator (OPO) was purchased as a supplemental tool for spectral characterization to be used in conjunction with an integrating sphere (IS). A more complex but similar setup has been realised before [2]. The addition of the new setup is motivated due to the following reasons:

1. The higher energy radiation of the laser driven OPO compared to the current setup will allow the use of an integrating sphere for spectral characterization such that several or all pixels can be characterized in short times.
2. The combination with the integrating sphere also will allow a simplified alignment of the spectroradiometer.
3. The shift of the maximum output toward the short wavelength range will allow better characterization of the spectroradiometer in the blue region of the spectrum, which is especially important for straylight characterization.

The goal of this paper is to present the expected performance of the new setup using data published from the OPO manufacturer and data measured at DLR. First the current setup is explained briefly, then the features of the OPO are described and how it is coupled to the integrating sphere. Afterwards the estimated performance of the combined OPO plus IS system is compared to two detector sensitivities and to the current setup.

2. CURRENT SETUP

The current setup is realized with a 100 W QTH lamp and a monochromator (Oriel MS257) as described in [1]. The setup has a minimum bandwidth of 0.13 nm in the spectral range from 0.2 - 1.4 µm and 0.25 nm in the range of 0.9 - 3 µm, calculated as slit width/dispersion for 40 mm slit width. The output from the monochromator is collimated with an off-axis parabolic mirror before it is directed onto the spectrometer. In order to fill the complete field of view (FOV) of the spectrometer to be characterized the exit slit of the monochromator is adjusted accordingly. This will lead to changes in bandwidth.

3. DESCRIPTION OF THE NEW SETUP

The new system consists of a tunable laser source, the laser pumped OPO, whose output is coupled into an IS. The spectroradiometer is mounted on top of the IS. A schematic of the setup is shown in figure 1.

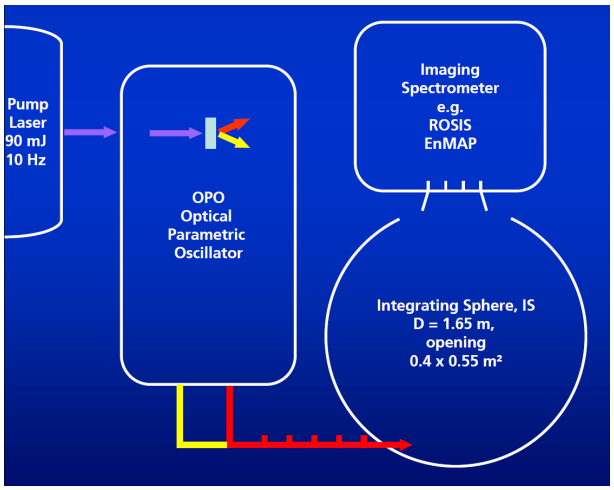

Figure 1. Schematic of the new setup.

3.1. The performance of the OPO

The optical parametric oscillator (OPO) uses a nonlinear crystal to generate two photons with lower energies from one single higher energy photon. The energies of the two newly generated photons are determined by the angle of the nonlinear crystal but must add up to the energy of the original photon ($h\nu_{\text{pump}}$) used:

$$h\nu_{\text{pump}} = h\nu_{\text{signal}} + h\nu_{\text{idler}} . \quad (1)$$

The higher energy light beam is called the signal ($h\nu_{\text{signal}}$) and the lower energy one is called the idler ($h\nu_{\text{idler}}$). The polarisation states of signal and idler are orthogonal to eachother. This process is known as parametric down conversion. The system planned to be employed (versaScan/120/MB) can be tuned for the signal beam from 405 nm to 709.4 nm, while the idler beam will change from 2550 nm to 709.4 nm at the same time. At 709.4 nm is the so called degeneracy point where the signal and the idler photons have the same energy. Due to the described process there always will be generated pairs of photons, whose energy add up to that of photons at 355 nm, the wavelength of the original photons from the pump laser (s. figure 2). The specified bidirectional repeatability for the wavelength step size is 0.05 nm. Since the nonlinear process in the optical crystal is a second order effect [3], one needs high numbers of photons to begin with. For that reason the OPO is driven by a pulsed high power laser at 355 nm wavelength (Spectra-Physics LAB-130-10). In order to further increase the efficiency of the parametric down conversion process the nonlinear crystal is placed into a resonant cavity forming the oscillator, leading to amplification. The overall efficiency of this process depends on the geometric and physical properties of the crystal and the cavity leading to wavelength dependence as shown in figure 2. The energy per pulse for the pump laser is 90 mJ. The pump laser and the OPO both operate at a pulse repetition frequeny of 10 Hz. The effect of the parametric down conversion on the bandwidth of the generated light pulses for signal and idler is shown in figure 3. The pulse width rises monotonically and quadratic from 0.07 nm at 410 nm to 2.7 nm at 2.6 µm.

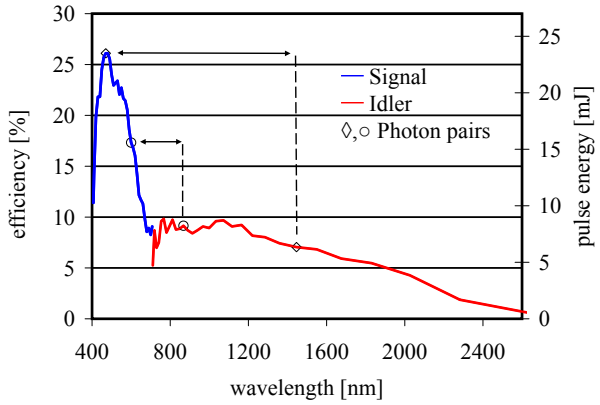

Figure 2. Conversion efficiency of the OPO for signal and idler wavelenghts. Right axis shows the respective pulse energy for a pump pulse of 90 mJ.

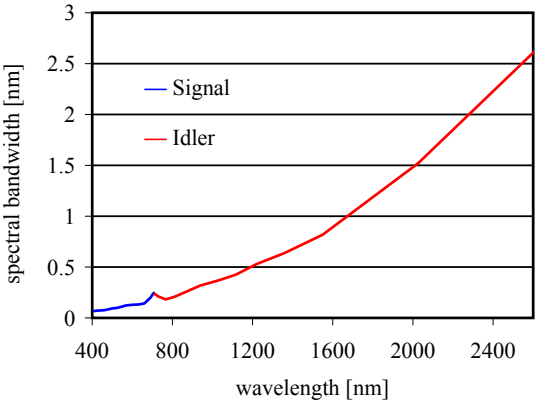

Figure 3. Bandwidth of the OPO for signal and idler wavelenghts.

3.2. Coupling the pulsed laser radiation to the IS

Depending on the wavelength required the signal or idler beam will be brought to the IS via free space reflective optics, keeping the optical path as short as possible. In this way the attenuation due to absorption in air, the change of pulse length and shape due to travel time and the line absorptions of aerial gases will be minimized. Short pathes also will increase safe handling of the radiation. Once the light reaches the IS it will be brought in by a port at the bottom of the sphere outside the FOV of the spectroradiometer to be characterized and directed towards the upper half of the IS. In this way it is assured that the laser radiation will be reflected and scattered several times before exiting the IS. The IS has a diameter

of 1.65 m and its inner surface is coated with $BaSO_4$, the reflectivity $\rho(\lambda)$ of which was measured on a sample as shown in figure 4. The IS transforms the directed laser pulse spatially into a homogeneous hemispherical light pulse and temporally by extending the duration of the pulse. The temporal shape of the exiting light is given by the convolution of the incoming light pulse and the exponential impulse response $R_{\mathrm{IS}}(t)$ (eq. 2). The dependence of the time constant $\tau(\lambda)$ of the impulse response on the wavelength (eq. 3) is shown in figure 5, where D_{s} is the diameter of the IS.

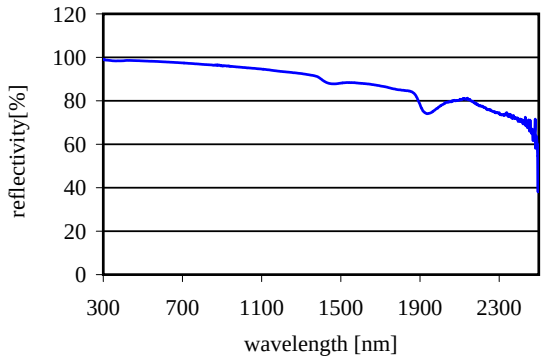

Figure 4. Reflectivity of the $BaSO_4$ used in the integrating sphere as measured from a sample.

$$R_{\mathrm{IS}}(t) = \exp\left(-\frac{t}{\tau(\lambda)}\right) \quad (2)$$

$$\tau(\lambda) = -\frac{2D_s}{3c\ln\rho(\lambda)} \quad (3)$$

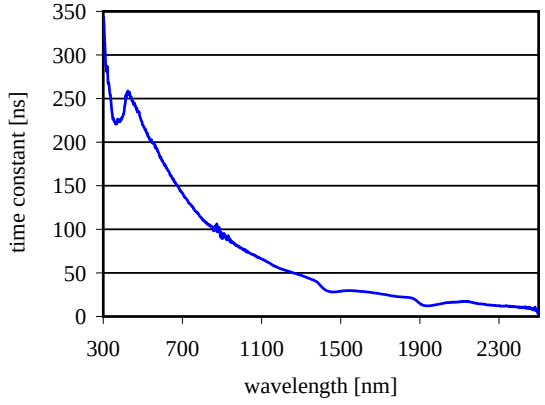

Figure 5. Time constant τ calculated from the reflectivity data as induced by the 1.65 m integrating sphere.

For comparison of the new setup with the current one and with imaging spectrometers, the spectral energy density per exiting light pulse $E_{\mathrm{out}}(\lambda)$, and an average spectral radiance $L(\lambda)$, using the pulse repetition frequency f, are calculated. In order to do so the spectral sphere multiplier (or sensitivity factor) $M(\lambda)$ is evaluated first. The measured reflectivity $\rho(\lambda)$, the ratio r_{A} of the exit port opening to the surface A_{sphere} of the IS, and the incremental wavelength $\Delta\lambda = 1\,\mathrm{nm}$ are used. E_{in} is the energy of a single incoming pulse coupled to the IS as calculated on the right hand side in figure 2.

$$M(\lambda) = \frac{\rho(\lambda)}{1-(1-r_A)\rho(\lambda)} \quad (4)$$

$$E_{\mathrm{out}}(\lambda) = \frac{M(\lambda)}{\pi\Delta\lambda A_{\mathrm{sphere}}}E_{\mathrm{in}} \quad (5)$$

$$L(\lambda) = E_{\mathrm{out}}(\lambda)f \quad (6)$$

4. USING THE NEW SETUP FOR FAST SPECTRAL CHARACTERIZATION

4.1. Comparing the exiting light pulse to the imaging spectrometer energies

The estimated ouput energy density per pulse $E_{out}(\lambda)$ can be compared to the energies required by the hyperspectral sensors ROSIS [4] and EnMAP (www.enmap.org). The spectral noise equivalent radiation (NER) and saturation levels were calculated from the measured ROSIS response, while EnMAP's levels were communicated privately. Figure 6 shows that the predicted energy per light pulse exiting from the IS is 1-2 magnitudes higher than the NERs over the complete spectral range. Using a pulsed illumination system will put a mild restriction on the scanning frequency of the spectrometer such that the scanning frequency should be more than twice as high as the laser repetition frequency in order to avoid multiple pulses per frame. Also frames from pulses reaching the detector array during the read-out phase need to be sorted out for the characterization process.

4.2. Comparing radiances of the new and the current setup

Using the 10 Hz pulse repetition frequency f as indicated by eq. 6, the radiance of the new system was calculated. The result is plotted in figure 7 together with single pixel measurements taken from the current continuously radiating setup using a portable spectrometer (ZEISS MCS 501). The envelope over the tops of these measurements gives an indication of the spectral radiance of the current system. The maximum of the envelope is around 700 nm,

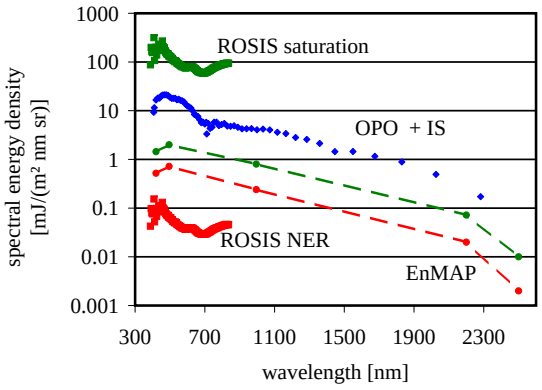

Figure 6. Energy per pulse calculated from measured data and in comparison to the noise equivalent radiation (NER) and saturation levels of ROSIS and EnMAP, as projected.

while the maximum of the estimated radiances of the new setup is around 470 nm, shifted towards the blue region of the visible part of the spectrum. In order to fully illuminate the pixel to be measured with the current setup the exit slit of the monochromator has to be adjusted accordingly. The width of the measured spectral features in figure 7 is between 4-6 nm. On the contrary the use of the IS in the new setup does not change the spectral bandwidth of the light pulse significantly, it is determined only by the OPO as shown earlier in figure 3 and which is below 0.5 nm in the visible.

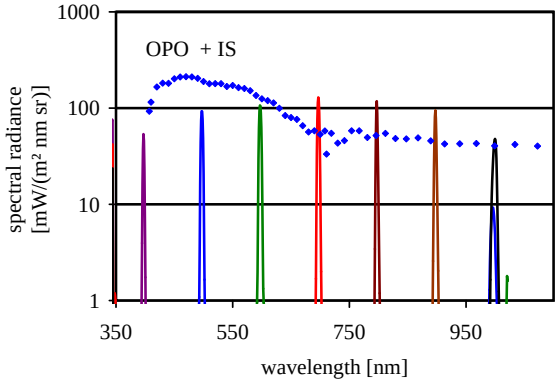

Figure 7. Average spectral radiance of OPO and integrating sphere setup as calculated (blue squares) compared to measured spectral radiance from current monochromator setup (colored lines).

5. CONCLUSIONS

The main advantages of the new OPO and integrating sphere system over the current single pixel monochromator setup is the possibility of complete FOV illumination allowing a faster and complete spectral characterization, a faster alignment of the imaging spectrometer and the shift of the maximum spectral radiance towards the blue. Similar as the current setup the new setup can not only be used for spectral characterization of the complete detector array of the spectrometer, but also for measurements of single pixel spectral response functions and for spectral straylight measurements [5].

ACKNOWLEDGEMENTS

The authors wish to thank P. Schötz for the measurement of the reflectivity of the $BaSO_4$ sample. Essential parts of the infrastructure of CHB as described above were funded by ESA under contract 16586/02/NL/GS.

REFERENCES

[1] Peter Gege, Jochen Fries, Peter Haschberger, Paul Schoetz, Horst Schwarzer, Peter Strobl, Birgit Suhr, Gerd Ulbrich, and Willem Jan Vreeling. Calibration facility for airborne imaging spectrometers. *ISPRS Journal of Photogrammetry and Remote Sensing*, 64(4):387–397, JUL 2009.

[2] Steven W. Brown, George P. Eppeldauer, and Keith R. Lykke. Facility for spectral irradiance and radiance responsivity calibrations using uniform sources. *APPLIED OPTICS*, Vol. 45, No. 32:8218 – 8237, 2006.

[3] Richard Lee Sutherland. *Handbook of Nonlinear Optics*. Marcel Dekker, 2003.

[4] P Gege, D Beran, W Mooshuber, J Schulz, and H van der Piepen. System analysis and performance of the new version of the imaging spectrometer ROSIS. In Schaepman, M and Schlapfer, D and Itten, K, editor, *1ST EARSEL WORKSHOP ON IMAGING SPECTROSCOPY*, pages 29–35, LAB TELEDETECT INRA-INA PG, 78000 VERSAILLES, FRANCE, 1998. EARSeL, EUROPEAN ASSOC REMOTE SENSING LABORATORIES. 1st EARSeL Workshop on Imaging Spectroscopy, ZURICH, SWITZERLAND, OCT 06-08, 1998.

[5] YQ Zong, SW Brown, BC Johnson, KR Lykke, and Y Ohno. Simple spectral stray light correction method for array spectroradiometers. *APPLIED OPTICS*, 45(6):1111–1119, FEB 20 2006.